A Feasibility Study on Microwave Imaging for Domestic Compost Production Monitoring

A Feasibility Study on Microwave Imaging for Domestic Compost Production Monitoring

1st David O. Rodriguez-Duarte
Dept. of Elec. and Telecomm.
Politecnico di Torino
Torino, Corso Duca degli Abruzzi 24
david.rodriguez@polito.it

2nd Melania Fiore
Dept. of Applied Science and Technology
Politecnico di Torino
Torino, Corso Duca degli Abruzzi 24
melania.fiore@polito.it

3rd Andrea De Simone
Dept. of Elec. and Telecomm.
Politecnico di Torino
Torino, Corso Duca degli Abruzzi 24
andrea.desimone@polito.it

4th Fabrizio Riente
Dept. of Elec. and Telecomm.
Politecnico di Torino
Torino, Corso Duca degli Abruzzi 24
fabrizio.riente@polito.it

5th Giovanna Turvani
Dept. of Elec. and Telecomm.
Politecnico di Torino
Torino, Corso Duca degli Abruzzi 24
giovanna.turvani@polito.it

6th Francesca Demichelis
Dept. of Applied Science and Technology
Politecnico di Torino
Torino, Corso Duca degli Abruzzi 24
francesca.demichelis@polito.it

7th Tonia Tommasi
Dept. of Applied Science and Technology
Politecnico di Torino
Torino, Corso Duca degli Abruzzi 24
tonia.tommasi@polito.it

8th Francesca Vipiana
Dept. of Elec. and Telecomm.
Politecnico di Torino
Torino, Corso Duca degli Abruzzi 24
francesca.vipiana@polito.it

***Abstract*—Home compost production requires regular monitoring of temperature and humidity, as well as interventions to ensure the correct maturation of the mass and high-quality compost. This article studies the adoption of microwave imaging (MWI) as a supporting tool to detect, locate, and monitor biomass hot spots, which are detrimental to the entire production. In this regard, it provides a threefold contribution: first, the dielectric characterization and temperature profiling of the compost; second, the introduction of a robust low-power wireless temperature sensor; finally, the validation of the MWI for retrieving the thermal profile of hot spots via 2-D numerical experiments, considering critical design aspects such as spatial resolution, operating frequency and number of wave probes. The proposed imaging technique combines information from a network of temperature sensors and scattered electromagnetic field samples to simplify the linear imagery-based strategy. Furthermore, the MWI system is supported by an electronic system equipped with temperature, humidity, and pH sensors to integrate the information and validate its functionality in the prototype phase. Overall, we demonstrate that it is feasible to use MWI for compost temperature monitoring.**

***Index Terms*—dielectric characterization, compost processing, multi-sensor electronic board, microwave imaging**

This study was carried out within the Agritech National Research Center and received funding from the European Union Next-GenerationEU (PIANO NAZIONALE DI RIPRESA E RESILIENZA (PNRR) – MISSIONE 4 COMPONENTE 2, INVESTIMENTO 1.4 – D.D. 1032 17/06/2022, CN00000022). This manuscript reflects only the authors' views and opinions, neither the European Union nor the European Commission can be considered responsible for them.

This study is also part of a PON PhD, funded by European Union FSE REACT-EU (PON Ricerca e Innovazione 2014-2020 - Asse IV, Azione IV.5 - Dottorati su tematiche green - DM 1061/2021)

I. Introduction

Compost is a key organic amendment for sustainable agriculture. Derived from various biomasses, organic amendments are rich in organic matter and nutrients, thereby enhancing soil fertility and promoting plant growth [1]. These products undergo specific processes to stabilize and sanitize the organic matter they contain, ensuring safe use. Composting is one of these processes. It results in a humus-like product of fine particles where the original material is no longer identifiable, the well-known compost.

Composting is a naturally occurring process that relies on anaerobic microorganisms to transform and stabilize solid organic matter. However, due to the lengthy and variable nature of the spontaneous natural process, it has been refined to be carried out in specialized facilities in a faster and more controlled way. In both cases, composting is exothermic, and the energy released is partly used by microorganisms and partly released as heat, increasing the temperature of the composting mass and making the temperature a distinctive indicator of different phases of the composting process. Moreover, pH is another important parameter that indicates the proper evolution of compost since it describes the proper environmental conditions for microorganisms. As the composting process proceeds, the degradation and volatilization of organic acids and the production of bases (e.g., ammonium, pyridine, pyrazine) increase pH.

The composting is a two-phase process. The initial mesophilic phase involves the rapid decomposition of easily

degradable organic matter. It releases significant thermal energy, which raises the temperature and accelerates the degradation rate, leading to the subsequent thermophilic phase, during which temperatures naturally rise above 70 °C. Such high temperatures reduce pathogenic agents in the material, ensuring the necessary stabilization and sanitization. The final phase, known as maturation, involves mineralizing hard-to-degrade molecules and humidifying lignocellulosic compounds. Hence, the degradation rate decreases during this phase, and the temperature drops [2]. The various phases are controlled in industrial facilities, but the process is mostly thermally self-regulated, thanks to the massive volumes involved. However, challenges arise when working with small volumes, like those in domestic and laboratory-scale systems, because compost mass no longer self-regulates crucial parameters such as temperature, humidity, and oxygen, which sporadically provokes the spike of hot spots within the composting mass, disrupting its adequate maturity. Thus, they must be identified and removed to avoid potential damage to the process. Nevertheless, the identification task is complex, as measuring the entire mass interior is challenging and procedurally inconvenient, using just a temperature sensor network or even a thermal camera. For the former, the network would take punctual measures, risking missing the hot spot, and for the latter, the camera would show just the temperature on the surface of the mass, therefore having a similar drawback. Overcoming this limitation, microwave imaging (MWI) is a promising non-ionizing, low-intensity, and cost-effective alternative to monitor the compost.

MWI is a widely used technology that exploits the penetration characteristics of microwaves to produce a contrast of dielectric maps, reflecting a variation within the studied scenario, from a limited number of electric field samples [3]. Therefore, it can be used to follow up the compost evolution, which is essential to understanding and optimizing the process. For instance, in the medical field, it is used to determine the variation between healthy and non-healthy tissues in breast cancer or brain stroke cases [4], [5], and in the food industry, to detect contaminants in packed food [6], or spoiled spots within storage grain silos [7]. Moreover, MWI is used to monitor soil water diffusion [8], and thermal variations [9], [10]. In the latter, MWI is used to indirectly report temperature variation, using the fact that the permittivity of water changes with the temperature [11].

Starting from the premise that hot spots in a composting mass present a dielectric contrast to their surroundings, this article continues [12], offering a preliminary validation of using a joined temperature sensor and MWI system, which provides real-time temperature profiles. This approach allows the detection of hot spots within the lightweight compost mass that could otherwise damage the home compost production, ensuring uniform, high-quality maturation. In the first part, we approach domestic compost production and its characterization using the open-coaxial probe method. The second part describes the electronics for automatically and continuously measuring temperature, humidity, and pH punctually. Finally, a numerical analysis evaluates the feasibility of an MWI, showing its capabilities to retrieve temperature maps over the whole domain.

II. Smart Composter

Based on the Smart Composter proposed in [12], we set up a domestic version using a 10-liter salad spinner, conveniently modified for the purpose. It was chosen for its internal colander, which allows the separation of leachate from the solid matrix, and for its cover, which enables the creation of a closed system for monitoring gas production and air supply. However, the process in this way was complex to manage, and a more naturally-driven system was chosen, even though this entailed the loss of control and possible data collection for gaseous flows. In this version, a thick-walled polystyrene box was chosen because it permits better insulation and lower thermal dispersion, thus helping to maintain the treated biomass at a convenient temperature. Holes were performed on the box walls for air circulation. Periodic inspections and mixing were made to monitor and eventually adjust humidity and make it uniform. We use a mixture of vegetable wastes and cow manure as feedstock material.

We use a low-cost ad-hoc board based on the electronic STM32 Nucleo from the WL family, integrated with waterproof sensors for temperature and humidity, S-TH-01 from Seed Studio, and a pH sensor, S-PH-01, placed in the middle of the compost pile. It continuously monitors the maturation of the composting mass and supports the imaging algorithm. It allows the collection of precise environmental data used as additional information that enhances and facilitates thermal profiling by the MWI system. The synergy between the MWI system and the electronic board guarantees a more robust functioning. The selected board, advantageously, integrates an antenna and an RF transceiver supporting the Long Range (LoRa) protocol. This allows us to develop an application to transmit data to a server using the LoRaWAN layer protocol. The sensors transmit the measured data using the Modbus protocol on a bus that follows the RS485 standard specification. This approach is chosen to create a system robust to electromagnetic noise, as the bus relies on differential communication. In this way, the system is less problematic when placed in an environment with several instruments, and long cables can be utilized. The system collects data every 30 minutes and sends it to a gateway connected to the internet. The gateway transfers the measurements to a server, which is accessible remotely. For this service, we rely on The Thing Network (TTN), which allows us to realize a LoRaWAN application for collecting small packets of data from a device with LoRa support. Figure 1 illustrates the system architecture.

The MWI part of the system has yet to be described since this article studies its feasibility and has not already been implemented. The following sections discuss details of its design and required features, as well as the optimization for reducing its overall complexity and, thus, also cost.

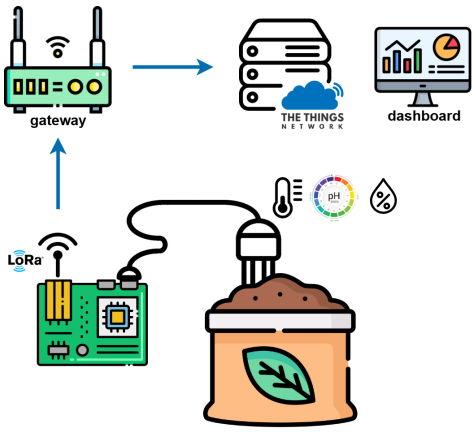

Fig. 1. Schematic representation of the automatic system for temperature, humidity and pH data collection.

III. Characterization

Considering there were no previous reports on the dielectric characterization of the compost at microwaves, to the best of the authors' knowledge, we start with a dielectric and temperature characterization of the compost that allows us to set numerical feasibility studies. Then, we focus on the electromagnetic evolution of compost over a month, starting around week six of the composting process when the mass exhibits uniform consistency. This premise allows us to assume a homogeneous distribution of the complex permittivity and the temperature and limit the span of the variables in this preliminary study.

The measuring procedure involves taking punctual measurements of temperature and reflection coefficients of the open coaxial probe at various points. For convenience, the temperature is measured directly on site, while nearby samples are taken to measure the reflection coefficients. The temperature measures are taken using the ad hoc system, which constantly

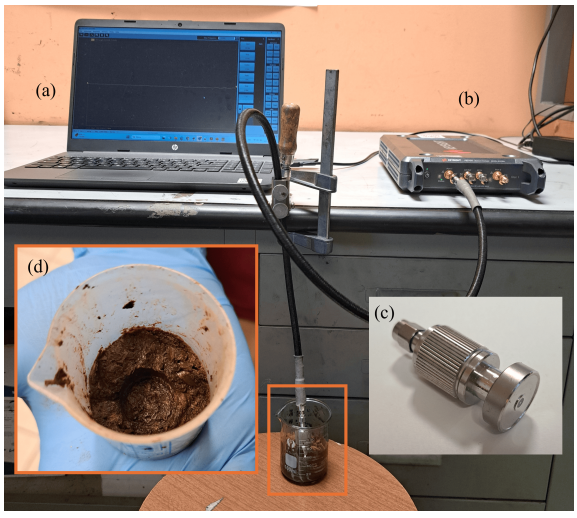

Fig. 2. Experimental setup for characterization. (a) Laptop, (b) Vector Network Analyzer, (c) Dielectric Probe, and (d) Compost sample.

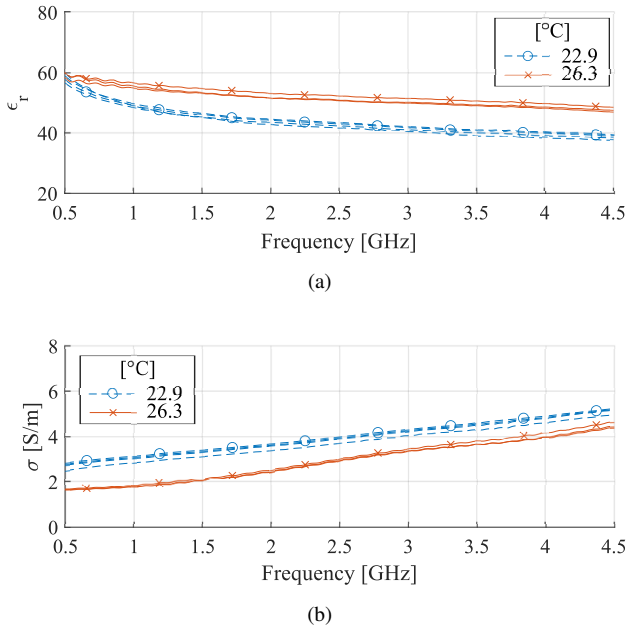

Fig. 3. Compost dielectric properties. (a) Permittivity; (b) Conductivity. The blue and red lines indicate measures at weeks six and eleven, respectively.

reports them, ensuring gradual monitoring of the changes. Meanwhile, we use the Agilent 85070D dielectric probe and the Keysight N5227A Vector Network Analyzer (VNA) for the reflection measures [13], [14], which we employ to retrieve the dielectric properties, i.e., permittivity and conductivity, ϵ_r and σ, respectively, of the material under test (MUT) in the microwave range. The experimental setup is shown in Fig. 2. Specifically, we obtain unknown MUT dielectric properties via the open coaxial probe method with a modal expansion at the probe tip that uses the lumped element model proposed in [15], which was proven to be accurate [16], [17]. To this end, we first measure the probe reflection coefficient in three known cases: i) air (open condition), ii) closed on a perfect electric conductor (short), and iii) immersed into distilled water (well-known load). Afterward, we measure the MUT, putting the probe in direct contact with the face of the sample, avoiding imperfections, and keeping constant pressure. The characterization is carried out at room temperature. Moreover, it is worth noticing that, unlike the temperature sensor, the probe is not aimed to work in prolonged and constant contact with a material like compost, which could ruin it.

Figure 3 reports the retrieved dielectric properties for two scenarios. The first one, week six, with a mass temperature of 22.9 °C, and the second one, week eleven, with a temperature of 26.3 °C. Because different samples were used on each day of the measuring campaign, the figure reports more than one line for each. However, the results clearly identify two different families, each for a study scenario, as expected from a homogeneous distribution.

IV. Microwave Imaging

MWI implies an inverse ill-posed and non-linear problem that aims to retrieve the dielectric contrast within the Domain of interest (DoI), reflecting the concentrated temperature drifts and representing the spotted physical changes. Hence, we can define the imaging like $\Delta\mathbf{E}^{\text{sct}} = \mathcal{L}(\Delta\chi)$, where $\mathcal{L}$, the kernel, is an integral operator that casts a dielectric contrast spatial map defined in the DoI, $\Delta\chi$, accounting for the variation at the considered time instant, with the sampled differential scattered field, $\Delta\mathbf{E}^{\text{sct}}$. However, assuming "weak" and localized contrast, like in the monitoring case of hot spots, the Kernel can be linearized using the Distorted Born approximation as follows [18]:

$$\Delta\mathbf{E}_{sct}(\mathbf{r}_p, \mathbf{r}_q; \omega) = \int_{\text{DoI}} \underline{\mathbf{G}}(\mathbf{r}_p, \mathbf{r}; \omega) \cdot \mathbf{E}^0(\mathbf{r}, \mathbf{r}_p; \omega) \Delta\chi_{sct}(\mathbf{r}) d\mathbf{r}, \tag{1}$$

where $\mathbf{r} \in$ DoI is the position, $\omega = 2\pi f$ is the angular frequency, $\Delta\mathbf{E}^n_{sct}$ is the differential scattered electric field sampled at the position of the receiving p prove when transmitting from the position at q prove. Moreover, $\underline{\mathbf{G}}$ represents the Green's function for an assumed reference scenario, $\mathbf{E}^0$ is the total field in the reference scenario, $\Delta\chi_{sct}$ indicates the variation affected with respect to the reference, and the symbol "$\cdot$" denotes the dot product. This kernel describes the response to a point source as a function of the observation position, forming the point-spread function (PSF) containing the description of the system [3]. However, the a-priori knowledge of the reference scenario is required to obtain the electric fields used to build the kernel. To this end, we use an in-house 2-D Finite Element Method (FEM) based electromagnetic solver and a simple reference model that contains the geometrical information of the problem, i.e., proves positioning and domain geometry features, and assumes a homogenous distribution of the dielectric properties. It is worth remarking, that this assumption considers the local nature of the scattering phenomenon, dominated by the variation of the contrast. Moreover, we set the permittivity values by taking as reference the values from a sample characterization, a valid practical measure in a real scenario.

Then, to invert and regularize the problem, we use a Truncated Singular Value Decomposition (TSVD) as shown in (2), which decomposes the discretized kernel in $\langle [u], [\sigma], [v] \rangle$, where σ_n, u_n and v_n are the n-th singular value, right and left singular vectors, respectively, while and truncates it at N, acting as a regularization parameter. Following the strategy in [18], we truncate it with a value that is slightly lower than the one corresponding to the change of slope of the singular value's spectrum, i.e., the ratio between the first and most significant singular value with the others. Finally, it is worth noticing that the retrieved contrast can be remapped to a temperature profile.

$$\Delta\chi_{\text{sct}} = \sum_{n=1}^{N} \frac{1}{\sigma_n} \left\langle \Delta\mathbf{E}^{\text{sct}}, u_n \right\rangle v_n. \tag{2}$$

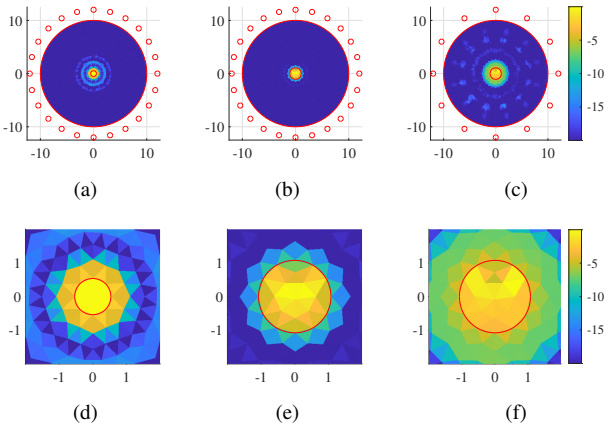

Fig. 4. Normalized projection of an ideal contrast point-like target truncating the operator at -30 dB. (a) $N_p = 24$, radio target:$\lambda/8$; (b) $N_p = 24$, radio target:$\lambda/4$; (c) $N_p = 12$, radio target:$\lambda/4$; (d-f) zoom-up views. Dimensions in [cm], and colormap in [dB].

V. Numerical Validation

To study feasibility, we perform a two-fold analysis using a 2-D simplified numerical version, which is a methodology that has been validated for other MWI applications, resulting in the baseline for implementing testing prototypes [19], [20]. In the first part, we evaluate the spatial resolution and the effect of the number of probes, and in the second one, we emulate a monitoring scenario. Specifically, we consider the DoI as a 10 cm-radio circumference, representing the compost container, surrounded by N_p transceiver field probes that, i.e., would act as transmitters or receptors assuming a multi-view configuration. In the experimental case, the probes are usually implemented using an array of antennas. For this assessment, we consider the probes to be immersed in a matching medium of the same material as the DoI, conveniently avoiding electrical discontinuities. This is a reasonable assumption that exploits the specifics of our problem from a practical point of view.

We defined the operation frequency as 1 GHz, considering that at this, first, the compost shows a clear contrast, and second, we will obtain a spatial resolution of about a $\lambda/4$ [21], [22], allowing us to detect centimetric variations. Moreover, knowing the resolution is also dictated by N_p, we test the system using either 12 or 24 probes.

A. Spatial Resolution Assessment

To assess the spatial resolution of the kernel, we evaluate the system PSF as in (3), which indicates the best possible retrieved contrast as the orthogonal projection of the contrast functions spanned by the first N right singular vectors [22].

Hence, it considers a point-like contrast scenario, setting a $\Delta\chi = 1$ in a point and $\Delta\chi = 0$ all the other points of DoI. Specifically, for the testing, we represent this point like either a circle with a radio of $\lambda/8$ or $\lambda/4$, around 0.5 and 1 cm at 1 GHz, respectively, placed in the middle of DoI, the worst

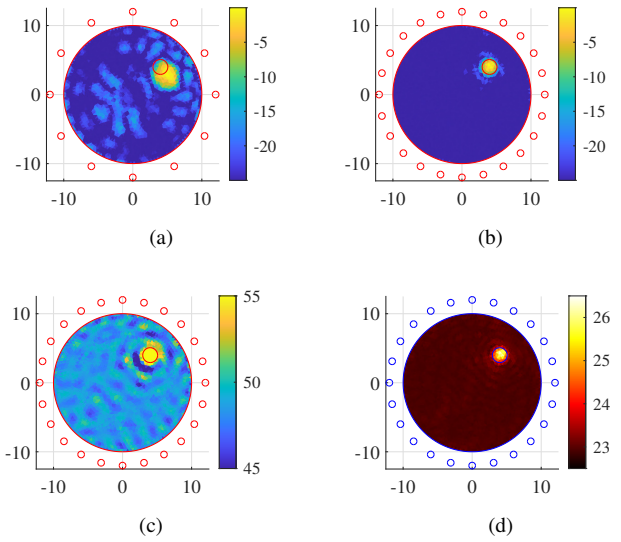

Fig. 5. Retrieved profiles. (a-b) Normalized $\Delta\chi$ [dB], (c) realive permittivity, ϵ_r, (d) Temperature [°C]. Dimensions in [cm].

scenario in term of penetration. Notice, that $\lambda/4$ is about the best expected resolution.

$$[\Pi_N] = \sum_{n=1}^{N} [v_n]\langle \cdot, [v_n]\rangle. \tag{3}$$

Figure 4 presents the normalized retrieved dielectric contrast in dB, considering in the first two columns, the cases using 24 probes, and in the third one using 12. The first column considers the $\lambda/8$ point-like contrast, and the last two, a $\lambda/4$ point-like contrast, both represented with a red contour line. From (a) and (d), and (b) and (e), one can notice the resolution is in the order of $\lambda/4$, assuming this as the values about -5 dB. Then, from (c) and (f), the case using 12 probes, the resolution remains. Though, the contrast shape is no so well defined. The case with a $\lambda/8$ contrast and 12 probes gets a similar response.

B. Temperature Monitoring

Finally, for the imaging testing, we select a contrast indicating a $\lambda/4$ hot spot with a temperature variation from 22.9 °C to 26.3 °C, i.e., from $\epsilon_r = 50$ and $\sigma = 3.2$ [S/m] to $\epsilon_r = 58$ and $\sigma = 1.9$ [S/m], at 1 GHz, respectively. The top row of Fig. 5 shows the normalized dielectric contrast using 12 probes in (a) and 24 in (b), noticing in the former a misleading of the contrast localization caused by the less amount of information. Meanwhile, the bottom row presents the retrieved real permittivity in (c) and the remapped temperature profile in (d).

The results demonstrate the feasibility of identifying the hot spots in the compost with a more precise resolution when 24 probes are used, which is relevant for understanding the process. However, a less complex system with fewer probes, thus, lower cost, would fulfill the requirements when it is considered a more practical scenario where detection is the key element, aside from exact localization or target shape definition, to prompt intervention consisting of injecting oxygen or moving the mass.

VI. Conclusion and Perspectives

This article evaluated the use of MWI to detect harmful hotspots in biomass during compost production in a domestic setting. First, he focused on the dielectric characterization of the compost and its correlation with the temperature and maturation stage, subsequently allowing a numerical analysis. Second, a wireless sensor network was proposed to provide a-priori temperature data during imaging. Finally, the usefulness of a non-iterative linear MWI algorithm as a physically informed inversion was validated, which recovers temperature contrast maps over the entire domain, i.e., the compost pile, improving the punctual measurements of the sensors and allowing the detection and monitoring of centimeter contrast variations. Furthermore, the use of an ad-hoc designed multi-sensor electronic board plays a crucial role in integrating the information coming from the sensors and in the validation of the functionality of the system in the prototype phase. In future work, we intend to extend the characterization of the compost, including the pH as a defining variable of the compost, that could be integrated as additional a-priori information into the inversion algorithm. Overall, this work is an ad-hoc solution and first step towards a low-cost alternative that supports sustainable home compost production.

Acknowledgments

We thank Eng. Martina Gugliermino for supporting the measuring campaign with the Department of Electronics and Telecommunications of Politecnico di Torino.

References

[1] R. Harrison, "Composting and formation of humic substances," in *Encyclopedia of Ecology*, S. E. Jørgensen and B. D. Fath, Eds. Oxford: Academic Press, 2008, pp. 713–719. [Online]. Available: https://www.sciencedirect.com/science/article/pii/B9780080454054002627

[2] U. Krogmann, I. Körner, and L. F. Diaz, *Composting: Technology*. John Wiley & Sons, Ltd, 2010, ch. 9.2, pp. 533–568. [Online]. Available: https://onlinelibrary.wiley.com/doi/abs/10.1002/9780470666883.ch35

[3] S. Doğu, D. Tajik, M. N. Akıncı, and N. K. Nikolova, "Improving the accuracy of range migration in 3-d near-field microwave imaging," *IEEE Transactions on Microwave Theory and Techniques*, vol. 71, no. 8, pp. 3540–3551, 2023.

[4] L. Guo, A. S. Alqadami, and A. Abbosh, "Stroke diagnosis using microwave techniques: Review of systems and algorithms," *IEEE Journal of Electromagnetics, RF and Microwaves in Medicine and Biology*, vol. 7, no. 2, pp. 122–135, 2022.

[5] E. Porter and D. O'Loughlin, "Pathway to demonstrating clinical efficacy of microwave breast imaging: Qualitative and quantitative performance assessment," *IEEE Journal of Electromagnetics, RF and Microwaves in Medicine and Biology*, vol. 6, no. 4, pp. 439–448, 2022.

[6] M. Ricci, J. A. T. Vasquez, R. Scapaticci, L. Crocco, and F. Vipiana, "Multi-antenna system for in-line food imaging at microwave frequencies," *IEEE Transactions on Antennas and Propagation*, vol. 70, no. 8, pp. 7094–7105, 2022.

[7] J. LoVetri, M. Asefi, C. Gilmore, and I. Jeffrey, "Innovations in electromagnetic imaging technology: The stored-grain-monitoring case," *IEEE Antennas and Propagation Magazine*, vol. 62, no. 5, pp. 33–42, 2020.

[8] X. Zhang, H. Tortel, S. Ruy, and A. Litman, "Microwave imaging of soil water diffusion using the linear sampling method," *IEEE Geoscience and Remote Sensing Letters*, vol. 8, no. 3, pp. 421–425, 2011.

[9] J. Redr, J. Vrba, T. Drizdal, R. Palmeri, R. Scapattici, and L. Crocco, "Microwave thermometry of brain tumors: A 2d computational feasibility study," in *2023 Photonics & Electromagnetics Research Symposium (PIERS)*. IEEE, 2023, pp. 1725–1731.

[10] M. Haynes, J. Stang, and M. Moghaddam, "Real-time microwave imaging of differential temperature for thermal therapy monitoring," *IEEE Transactions on Biomedical Engineering*, vol. 61, no. 6, pp. 1787–1797, 2014.

[11] A. Andryieuski, S. M. Kuznetsova, S. V. Zhukovsky, Y. S. Kivshar, and A. V. Lavrinenko, "Water: Promising opportunities for tunable all-dielectric electromagnetic metamaterials," *Scientific Reports*, vol. 5, no. 1, p. 13535, Aug 2015. [Online]. Available: https://doi.org/10.1038/srep13535

[12] G. Turvani, M. Fiore, D. O. Rodriguez-Duarte, F. Demichelis, T. Tommasi, F. Vipiana, and F. Riente, "Enabling high-quality compost for a smart domestic production," in *2023 IEEE International Workshop on Metrology for Agriculture and Forestry (MetroAgriFor)*, 2023, pp. 837–841.

[13] "Keysight N1501A dielectric probe kit 10 MHz to 50 GHz, technical overview," Accessed on: Dec. 11, 2020. [Online]. Available: https://www.keysight.com/it/en/assets/7018-04631/technical-overviews/5992-0264.pdf.

[14] "Streamline series vector network analyzer," Available at https://www.keysight.com/us/en/products/network-analyzers/streamline-series-usb-vector-network-analyzers/p50xxb-streamline-series-vector-network-analyzers.html.

[15] M. Stuchly and S. Stuchly, "Coaxial line reflection method for measuring dielectric properties of biological substances at radio and microwave frequencies," *IEEE Trans. Instrum. Meas.*, vol. 29, no. 3, p. 176–182, 1980.

[16] A. Tieri, S. Pisa, E. Piuzzi, F. Frezza, and M. Cavagnaro, "Wideband measurement of dielectric properties of wheat flour," *IEEE Transactions on Instrumentation and Measurement*, vol. 72, pp. 1–9, 2023.

[17] M. Cavagnaro and G. Ruvio, "Numerical sensitivity analysis for dielectric characterization of biological samples by open-ended probe technique," *Sensors*, vol. 20, no. 13, 2020.

[18] R. Scapaticci, L. Di Donato, I. Catapano, and L. Crocco, "A feasibility study on microwave imaging for brain stroke monitoring," *Progress In Electromagnetics Research B*, vol. 40, pp. 305–324, 2012.

[19] J. A. Tobon Vasquez, R. Scapaticci, G. Turvani, G. Bellizzi, N. Joachimowicz, B. Duchêne, E. Tedeschi, M. R. Casu, L. Crocco, and F. Vipiana, "Design and experimental assessment of a 2d microwave imaging system for brain stroke monitoring," *International Journal of Antennas and Propagation*, vol. 2019, pp. 1–12, 2019.

[20] D. O. Rodriguez-Duarte, C. Origlia, J. A. T. Vasquez, R. Scapaticci, L. Crocco, and F. Vipiana, "Experimental assessment of real-time brain stroke monitoring via a microwave imaging scanner," *IEEE Open Journal of Antennas and Propagation*, vol. 3, pp. 824–835, 2022.

[21] M. Slaney, A. Kak, and L. Larsen, "Limitations of imaging with first-order diffraction tomography," *IEEE Transactions on Microwave Theory and Techniques*, vol. 32, no. 8, pp. 860–874, 1984.

[22] R. Scapaticci, J. Tobon, G. Bellizzi, F. Vipiana, and L. Crocco, "Design and numerical characterization of a low-complexity microwave device for brain stroke monitoring," *IEEE Transactions on Antennas and Propagation*, vol. 66, no. 12, pp. 7328–7338, 2018.